Avrupa Bilim ve Teknoloji Dergisi
Özel Sayı 47, S. 79-84, Ocak 2023
© Telif hakkı EJOSAT'a aittir
Araştırma Makalesi

www.ejosat.com ISSN:2148-2683

European Journal of Science and Technology
Special Issue 47, pp. 79-84, January 2023
Copyright © 2023 EJOSAT
Research Article

Robust and accurate photoelectric system model design using the small-signal principle

Siham Aissani [1*], Mohcene Bechouat [2], Moussa Sedraoui [3], Toufik Amieur[4]

[1*] Université 8 Mai 1945 Guelma, Guelma, Algeria , Département Électronique et Télécommunications/ Laboratoires des Télécommunications LT de Guelma, (ORCID: 0000-0002-4900-2336), aissanisiham24@gmail.com
[2] Université de Ghardaïa, Algeria, Département d'automatique et d'électromécanique, Faculté dessciences et de la technologie,(ORCID: 0000-0002-0434-4324), mohcene.oui@gmail.com
[3] Université 8 Mai 1945 Guelma, Guelma, Algeria , Département Électronique et Télécommunications/ Laboratoires des Télécommunications LT de Guelma, (ORCID: :0000-0002-4590-2249), sedraoui.moussa@univ-guelma.dz,
[4] Département de Génie Électrique /Université de Larbi Tebessi Tebessa, Algeria, (ORCID: 0000-0003-0870-5446), amieur.to@gmail.com

(2nd International Conference on Innovative Academic Studies ICIAS, January 28 - 31, 2023)

(**DOI:** 10.31590/ejosat.1244942)

ATIF/REFERENCE: Aissani, S., Bechout, M., Sedraoui, M. & Amieur, T. (2023). Robust and accurate photoelectric system model design using the small-signal principle. *European Journal of Science and Technology*, (47), 79-84.

Abstract

Due to the importance of modeling and the urgent need for it in various applications, the design of an accurate model that simulates and is compatible with the real system to carry out various studies correctly, this has become a great challenge for researchers. Therefore, this research proposes the design of a mathematical model using the method of the small signal of the photovoltaic system consisting of the photovoltaic panel KC200GT feeding the load Through a DC-DC converter. This modeling method converts the mathematical model of the DC-DC converter from nonlinear behavior to linear behavior given in the state space formula, then the application of the Laplace transform will be used to obtain the transfer function. The latter is used in the studies to design the MPP controller. The simulation results showed that the modeling method based on the small signal method enables us to obtain an efficient and accurate model that is compatible with the real system and shows this compatibility in the voltage and energy between them.

Keywords: PV panel; DC-DC Boost converter; Maximum Power Point Tracking MPPT; small-signal.

---

[*] Corresponding Author: *aissanisiham24@gmail.com*

1. Introduction

The very negative impact of fossil fuels and their derivatives on all living organisms and on the environment has pushed researchers to find an alternative to them, namely renewable and natural energies, which are pure and economical, the most important of which is solar energy. It is operated with the help of a photovoltaic device consisting of its photovoltaic cells which have the ability to convert sunlight directly into electricity, a DC-DC step-up power converter, and a resistive load; The main objective is as follows: despite the change of weather (temperature and lighting), the output voltage of the load must be maintained at a constant value. This can be achieved by fabricating an MPPT maximum power point tracking controller, which uses the voltage and current generated by the PV system to provide the optimal α* cycle feeding the DC-DC converter. The design of a powerful MPP controller requires the use of an accurate linear model that accurately describes the behavior of the photovoltaic cell, so the behavior of the latter must be converted from non-linear to linear around the balance point, and given the importance of the process of modeling photovoltaic systems and the urgent need to design models that accurately simulate real systems prompt researchers to conduct research And several studies, including: Almeida et al. (2017) a comparative study of PV predictions using parametric and non-parametric PV models, where parametric modeling considers the PV system as a white box where each subsystem or component is modeled using a set of physical parameters and equations. While nonparametric modeling considers the PV system as a black box, assuming there is no information about the internal properties and processes of the PV system. Using a historical time series of inputs and outputs, the behavior of the photovoltaic system is estimated [1]; Wang Qiu (2020) et al. proposed a modeling method based on matrix variables for a distributed grid-connected PV system. The central idea of the modeling method is to simplify the complex model containing many PV-DCO generating units and turn it into an average two-unit model.

In this paper, the modeling process is done using the small signal method, which is an easy method that enables us to obtain an accurate model. The simulation results showed that the obtained model is consistent with the real system.

This paper is organized as follows. In the first section, the introduction is given, and then in the second section it is about photovoltaic modeling. In Section 3, the photovoltaic system is modeled using the small-signal principle. In Section 4, the photovoltaic system was validated using Matlab®/Simulink software. Finally, conclusions are drawn in Section 6.

2. Modeling of solar cells and electrical characteristics of the PV module

The electric cell can be represented by the electric model shown below

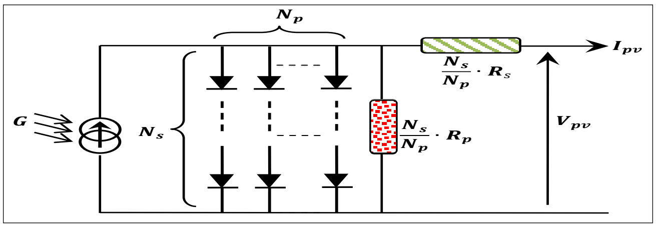

Fig. 1. Equivalent electrical circuit of the PV panel model

The i × v characteristic equation describing the single-diode model is shown in Fig. 1:

$$I_{pv} = N_p I_{ph} - N_p I_0 \left[\exp\left(\frac{\frac{V_{pv}}{N_s} + \frac{R_s I_{pv}}{N_p}}{aV_t} \right) - 1 \right] - \frac{\frac{N_p V_{pv}}{N_s} + R_s I_{pv}}{R_p} \qquad (1)$$

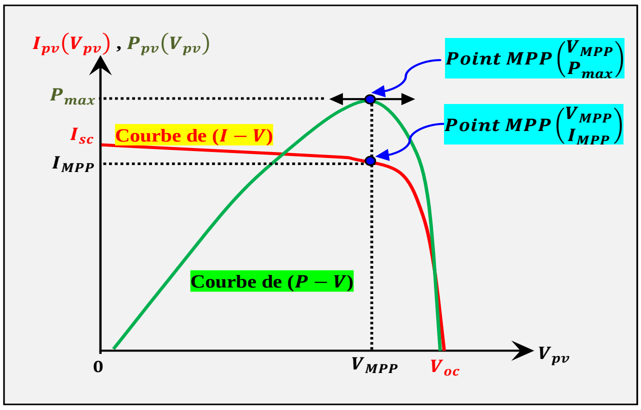

Fig. 2. Nonlinear i × v characteristic of the KC200GT solar panel and linear MPP equivalent model

Where T is the temperature of the PV cells constant, R_s is the equivalent series resistance, q is the electronic charge and k is the Boltzmann, $V_t = N_c kT / q$ is the thermal voltage, N_c is the number of cells connected in series, N_s and N_p are series and parallel string respectively, I_{Pv} and I_0 are the photovoltaic (PV) currents and saturation, a is the ideality constant of the diode, R_p is the equivalent shunt resistance.

This equation is at the origin of the I-V curve of figure 2, we note the points of interest which are the maximum power P-mpp, the voltage V-mpp at the maximum point, the current I-mpp at the maximum point.

We derive the non-linear curve at the point MPP, the photovoltaic panel becomes linear, i.e. the nominal curve i × v becomes linear, when differentiating we get:

$$g(V_{MPP}, I_{MPP}) = -\frac{N_P I_0}{N_s a V_t} \exp\left(\frac{V_{MPP}}{N_s a V_t} + \frac{R_s I_{MPP}}{N_P a V_t} \right) - \frac{N_P}{N_s R_p} \qquad (2)$$

The linear model obtained at the linear point is represented by the tangent of the curve i × v :

$$I_{pv} = gV_{pv} + \left(I_{MPP} - gV_{MPP}\right) \quad (3)$$

At the MPP point we represent PV In the equivalent circuit FIG 3 The constituent elements of Req and V_{MPP} :

$$R_{eq} = -\frac{1}{g}, \mathrm{V}_{eq} = \mathrm{V}_{MPP} + R_{eq} I_{MPP} \qquad (4)$$

Figure 3 represents the photovoltaic generator circuit at the linear point (V, I). At this point, we get the weak signal pattern. It is desirable that the operating point should always be near the maximum point MPP, no matter how the climatic conditions change, so a controller must be designed to ensure the optimum work of the photovoltaic system

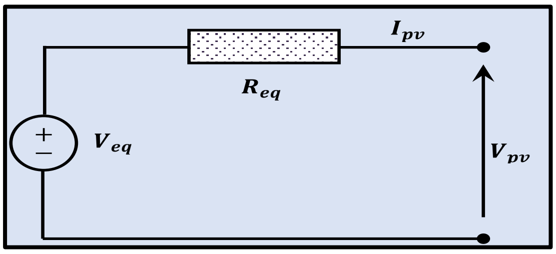

Fig. 3. Linear equivalent circuit valid for point linearization

The performance of a solar PV system depends on climatic conditions: Irradiation and temperature (ambient temperature) (Garcia, O., and others 2013).
The characteristics of photovoltaic cells change with weather conditions, temperature and solar radiation

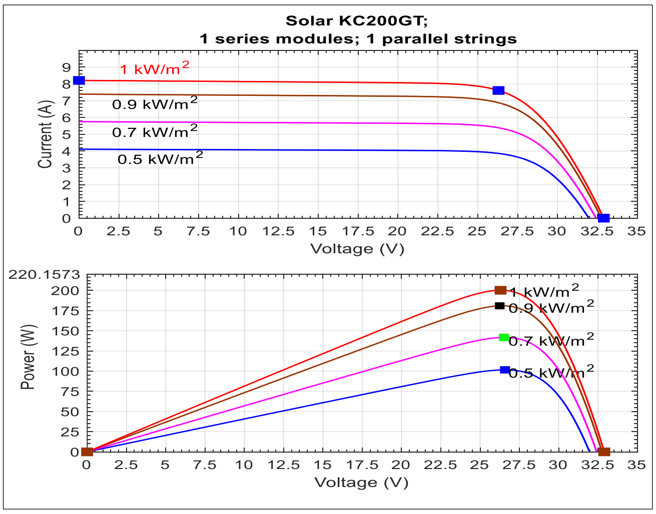

Fig.4. Characteristics (I-V) and (P-V) for variable G and T_n=25℃

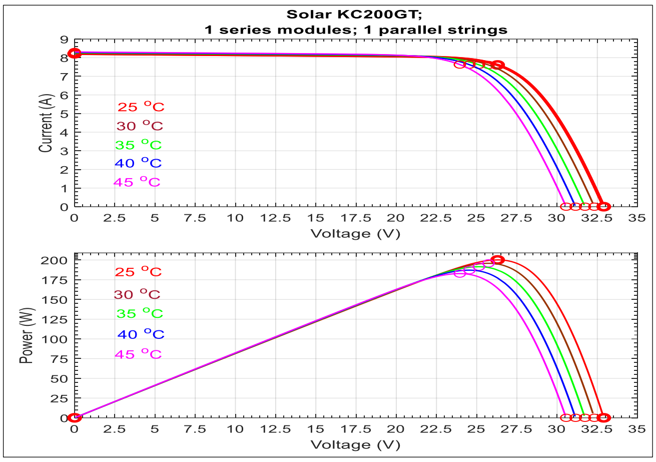

Fig.5. Characteristics (I-V) and (P-V) for variable T and G_n=1000W·m^{-2}

3. Modeling of global soLlar system

In general, most real-world applications require more power than the one generated by the basic KC200GT panel. Therefore, the introduction of the DC-DC boost converter becomes essential between it and the electrical device to be powered. Therefore, Fig.2 shows the equivalent electrical circuit describing the interconnection system including the KC200GT panel, the DC-DC boost converter and the resistive load.

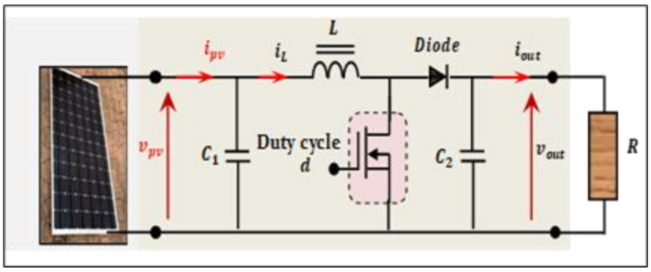

Fig.6. Interconnection system including the PV, DC-DC boost and the resistive load

According to Fig.6, it is easy to determine the nonlinear state space representation of the global MPPT scheme as below

$$\begin{aligned} \frac{d}{dt} v_{pv}(t) &= \frac{1}{C_1} i_{pv}(t) - \frac{1}{C_1} i_L(t) \\ \frac{d}{dt} i_L(t) &= \frac{1}{L} v_{pv}(t) - \frac{1-d}{L} v_{out}(t) \qquad (5) \\ \frac{d}{dt} v_{out}(t) &= \frac{1-d}{C_2} i_L(t) - \frac{1}{RC_2} v_{out}(t) \end{aligned}$$

When calculating the small-signal model from a state-to-state representation, given by Eq.5 even if the switching harmonics of the Boost DC-DC converter are removed, the averaged model result is still non-linear. It is therefore necessary to apply the principle of small signals according to the following steps:

State vector and variable inputs are defined for the global model.

- the operating point around which the linearization must be carried out are defined, ie the MPP supplied to STC.

•Disturbances, that is to say small variations, are introduced into all the inputs of the model, which leads to disturbances in all the state variables of the global model.

• The high frequency terms, the continuous and nonlinear terms are removed and only the disturbed components are kept. As a consequence, the average representation of the state space of the global model is given by considering only these perturbed components.It is important to mention that the perturbation applied to each state variable is given as follows:

$$\begin{aligned} V_{pv}(t) &= \mathrm{V}_{pv_{MPP}} + \delta V_{pv}(t) \\ i_L(t) &= I_{L_{MPP}} + \delta i_L(t) \\ V_{out}(t) &= \mathrm{V}_{out_{MPP}} + \delta V_{out}(t) \\ d(t) &= D_{MPP} - \delta d(t) \\ i_{pv}(t) &= \mathrm{I}_{MPP} + \delta i_{pv}(t) \end{aligned} \quad (6)$$

Where the sigma variable i.e. δx(t) is the disturbance value added to the constant steady state value X_MPP of the state variable X(t)

$$\begin{aligned} \frac{d}{dt}\left(V_{MPP} + \delta V_{pv}\right) &= \frac{1}{C_1}\left(I_{MPP} + \delta i_{pv}\right) - \frac{1}{C_1}\left(I_{LMPP} + \delta i_L\right) \\ \frac{d}{dt}\left(I_{L_{MPP}} + \delta i_L\right) &= \frac{1}{L}\left(V_{MPP} + \delta V_{pv}\right) - \frac{1-(D_{MPP}+\delta d)}{L}\left(V_{outMPP} + \delta V_{out}\right) \\ \frac{d}{dt}\left(V_{outMPP} + \delta V_{out}\right) &= \frac{1-(D_{MPP}+\delta d)}{C_2}\left(I_{L_{MPP}} + \delta i_L\right) - \frac{1}{R.C_2}\left(V_{outMPP} + \delta v_{out}\right) \end{aligned}$$

(7)

We eliminate the constant values and obtain the linear state-space representation of the photovoltaic system

$$\begin{bmatrix} \frac{d}{dt}\delta v_{pv}(t) \\ \frac{d}{dt}\delta i_L(t) \\ \frac{d}{dt}\delta v_{out}(t) \end{bmatrix} = \begin{bmatrix} -\frac{1}{R_{eq}C_1} & -\frac{1}{C_1} & 0 \\ \frac{1}{L} & 0 & \frac{1-D_{MPP}}{L} \\ 0 & \frac{1-D_{MPP}}{C_2} & -\frac{1}{RC_2} \end{bmatrix} \begin{bmatrix} \delta V_{pv}(t) \\ \delta i_L(t) \\ \delta V_{out}(t) \end{bmatrix} + \begin{bmatrix} 0 \\ -\frac{V_{out_{MPP}}}{L} \\ \frac{I_{L_{MPP}}}{C_2} \end{bmatrix} \delta d(t) \quad (8)$$

We apply the Laplace transform using the values given in the following data table we find the following transfer function G(s):

$$G(s) = \frac{1.683\mathrm{e}08.s + 5.609e08}{s^3 + 65.67s^2 + 5.464e05.s + 1.808e06} \quad (9)$$

4. Simulation results and discussion Validation of the photovoltaic system model based on the small signal principle Using Matlab®/Simulink Software

Table 1. system data

	Parameter		Value	Unit
KC200GT panel		I_0	9.825×10^{-8}	*A*
		I_{sc}	8.214	*A*
		V_{oc}	32.9	*V*
		a	1.3	-
		R_p	415.405	Ω
		R_s	0.221	Ω
		N_c	54	-
		N_s	1	-
		N_p	1	-
	Simplified circuit	V_{eq}	51.597	*V*
		R_{eq}	3.3242	*Ω*
	PV Parameters given at MPP	V_{MPP}	26.3	*V*
		$V_{out_{MPP}}$	316.34	*V*
		I_{MPP}	7.61	*A*
		D_{MPP}	0.91686	-
DC − DC boost converter	L		0.4	*mH*
	C_1		4700	*μF*
	C_2		1200	*μF*
Resistive load	R		500	*Ω*

Using the transfer function and MATLAB, we find photovoltaic system Bode Diagram:

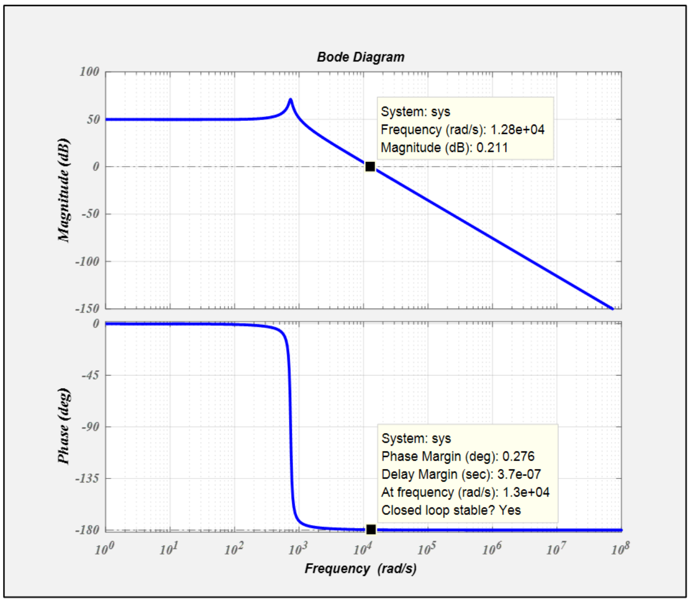

Fig7. Boost Converter Bode Diagram

$K_p = 0.002607$

$Ki = 8.15$ (10)

$K_d = 2.082 \times 10^{-5}$

The obtained linear model is verified with matlab; Figure 8 shows the output voltages of the real system V_{real} and the output voltages of the model V_{mod} based on the principle of the small signal that is modeled in this paper for the photovoltaic system consisting of a photovoltaic panel KC200GT, a Boost DC-DC converter - and a resistive load.

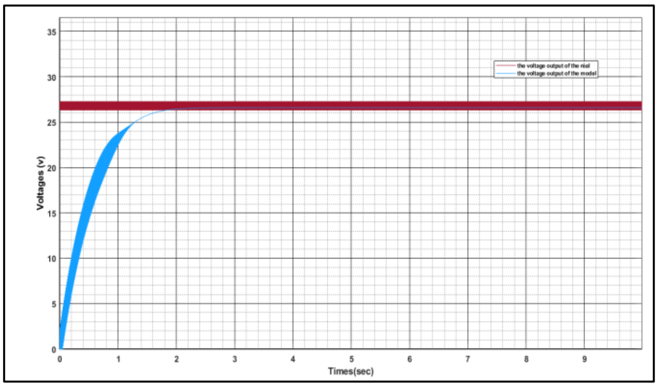

Fig.8.shows the output voltages of the real system V_{real} and the output voltages of the model V_{mod} based on the principle of the small signal

The obtained linear model is verified with matlab; Figure 9 shows the output power of the real system P_{real} and the output power of the model P_{mod} based on the principle of the small signal that is modeled in this paper for the photovoltaic system consisting of a photovoltaic panel KC200GT, a Boost DC-DC converter - and a resistive load.

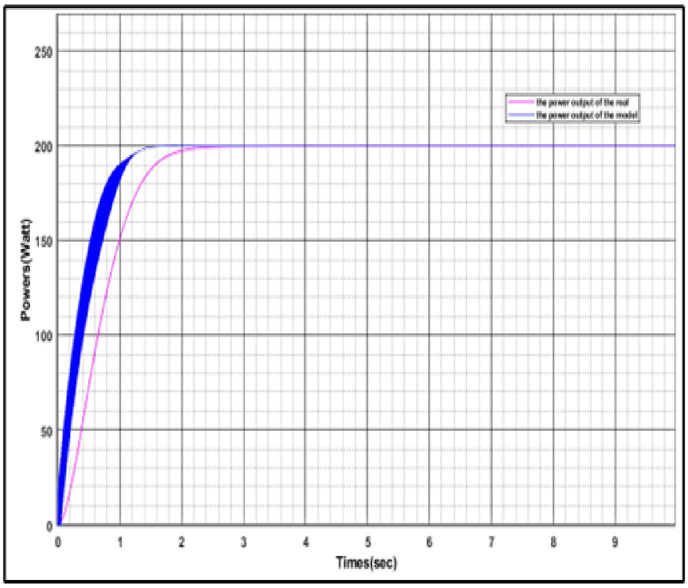

Fig.9.shows the output power of the real system P_{real} and the output power of the model P_{mod}

Simulation results show that the voltage and power produced by the model based on the small signal model, which has been Simulation results show that the voltage and power produced by the model based on the small signal model, which has been modeled in this paper, are almost equal to the voltage and power produced by the real system.

5. Conclusions and Recommendations

In this paper, the principle of small-signal modeling of the photovoltaic system consisting of the KC200GT photovoltaic panel feeding the Boost DC-DC converter and converting the nonlinear behavior of the system into a linear behavior near the equilibrium point is studied and discussed; We obtain a model that is more accurate and compatible with the real system than other modeling methods, and this is shown by the simulation results. This linear model will be used later in designing an effective MPP controller that guarantees good and excellent tracking dynamics for MPP.

References

[1] Almeida, M. P., Muñoz, M., de la Parra, I., & Perpiñán, O. (2017). Comparative study of PV power forecast using parametric and nonparametric PV models. *Solar Energy*, *155*, 854-866.

[2] Wang, Q., Yao, W., Fang, J., Ai, X., Wen, J., Yang, X., ... & Huang, X. (2020). Dynamic modeling and small signal stability analysis of distributed photovoltaic grid-connected system with large scale of panel level DC optimizers. *Applied Energy*, *259*, 114132.

[3] Dolara, A., Leva, S., & Manzolini, G., (2015), Comparison of dif ferent physical models for PV power output prediction. Solar energy, 119: 83-99.

[4] Villalva, M. G., De Siqueira, T. G., & Ruppert, E. (2010). Voltage regulation of photovoltaic arrays: small-signal analysis and control design. IET Power Electronics, 3(6), 869-880

[5] Kollimalla, S. K., & Mishra, M. K. (2014). A novel adaptive P&O MPPT algorithm considering sudden changes in the irradiance. IEEE Transactions on Energy conversion, 29(3), 602-610.

[6] Harrag, A., & Messalti, S. (2015). Variable step size modified P&O MPPT algorithm using GA-based hybrid offline/online PID controller. Renewable and Sustainable Energy Reviews, 49, 1247-1260.

[7] Althobaiti, A., M. Armstrong, and M. A. Elgendy. "Space vector modulation current control of a three-phase PV grid-connected inverter." 2016 Saudi Arabia Smart Grid (SASG). IEEE, 2016.

[8] Lasheen, M., Rahman, A. K. A., Abdel-Salam, M., & Ookawara, S. (2017). Adaptive reference voltage-based MPPT technique for PV applications. IET Renewable Power Generation, 11(5), 715-722.

[9] Aidoud, M., Feraga, C. E., Bechouat, M., Sedraoui, M., & Kahla, S. (2019). Development of photovoltaic cell models using fundamental modeling approaches. Energy Procedia, 162, 263-274.

[10] Dehghanzadeh, A., Farahani, G., Vahedi, H., & Al-Haddad, K. (2018). Model predictive control design for DC-DC converters applied to a photovoltaic system. International Journal of Electrical Power & Energy Systems, 103, 537-544.

[11] Palanisamy, R., Vijayakumar, K., Venkatachalam, V., Narayanan, R. M., Saravanakumar, D., & Saravanan, K. (2019). Simulation of various DC-DC converters for photovoltaic system. International Journal of Electrical and Computer Engineering, 9(2), 917.

[12] Bechouat, M., Younsi, A., Sedraoui, M., Soufi, Y., Yousfi, L., Tabet, I., & Touafek, K. (2017). Parameters identification of a photovoltaic module in a thermal system using meta-heuristic optimization methods. International Journal of Energy and Environmental Engineering, 8(4), 331-341.

[13] Ismail, M.S., Moghavvemi, M., & Mahlia, T.M.I., (2013). Characterization of PV panel and global optimization of its model parameters using genetic algorithm. Energy Conversion and Management, 73:10-25.